Angio-OCT: presente e futuro

Studio Oculistico
dott. A. Lucente
Inoculis salus

www.amedeolucente.it

Disclosure

Consulting Free

- Carl Zeiss Meditec
- Alfa Intes

LASERLAB Amsterdam

Optics in Medicine

Eye = 0.1mm
MO = 0,2 µm
ME = 0,2 nm

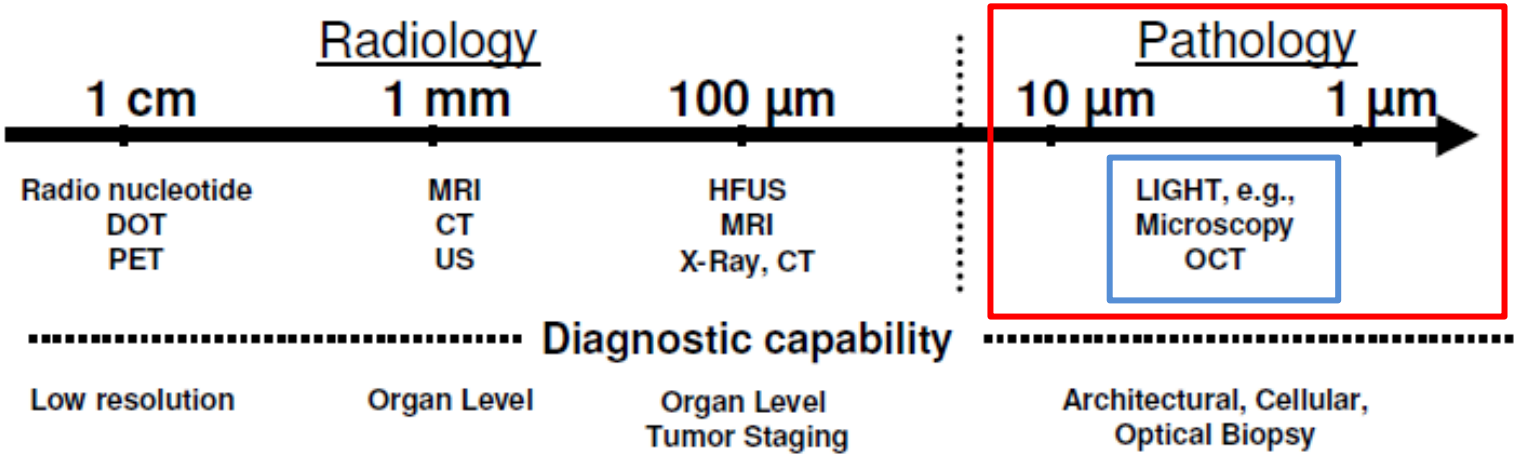

Histopathology is the golden standard especially for cancer diagnosis

Only optical technique approach cellular resolution

DOT: Diffuse Optical Tomography; PET: Positron Emission Tomography;
MRI Magnetic Resonance Imaging; CT: Computed Tomography; US: Ultra Sound;
HFUS: High Frequency Ultra Sound; OCT: Optical Coherence Tomography.

Algoritmo

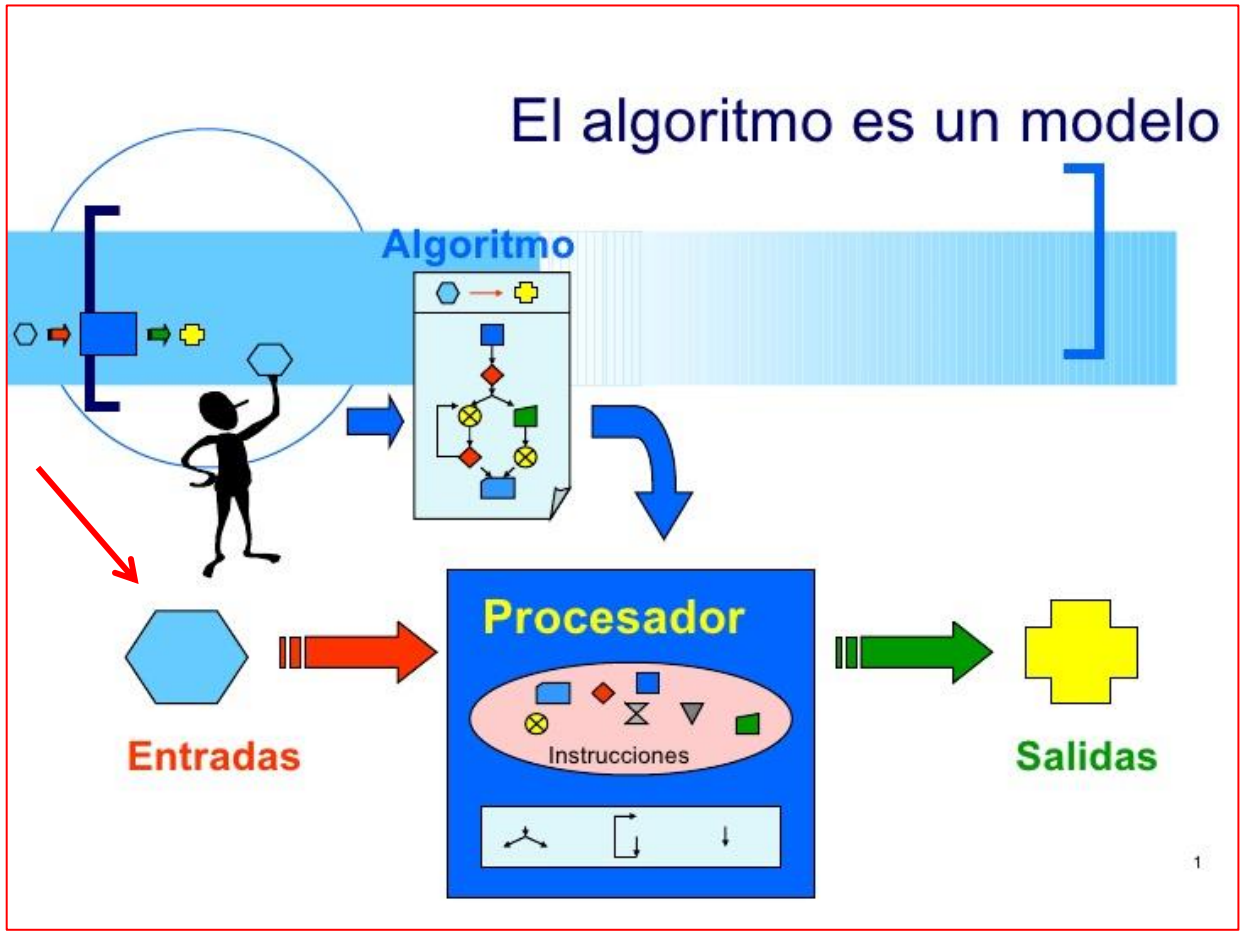

al-Khwarizmi محمد خوارزمی

(Corasmia o Baghdad, 780 – 850 d C circa)

Un algoritmo è un procedimento che risolve un determinato problema attraverso un numero finito di passi elementari in un tempo finito dal nome del matematico persiano al-Khwarizmi محمد خوارزمی inventore numero Zero

SSADA (brevetto WO 2014040070 A1, priorità 10 set 2012, David Huang et al.)

lab at Oregon Health & Science University
3375 SW Terwillinger Blvd Portland, OR 97239

Casey Eye Institute

SSADA **S**plit-**S**pectrum **A**mplitude-**D**ecorrelation **A**ngiography

Decorrelazione (decorrelation): è un processo matematico utilizzato nell'elaborazione dei segnali per modificare l'autocorrelazione (comparazione del segnale con se stesso) o le correlazioni incrociate (cross-correlazioni, comparazione delle immagini nel tempo), al fine di preservare alcune caratteristiche ed esaltarle

Decorrelazione dyeless del segnale tomografico

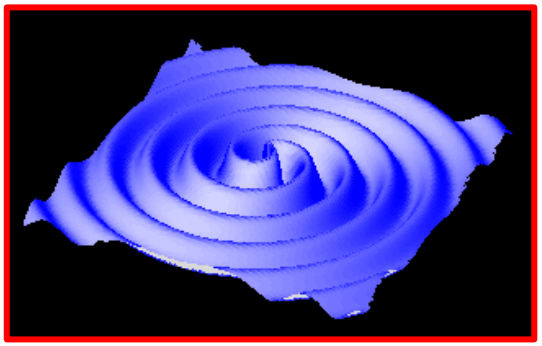

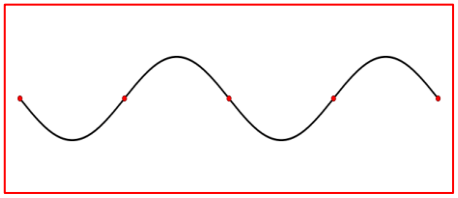

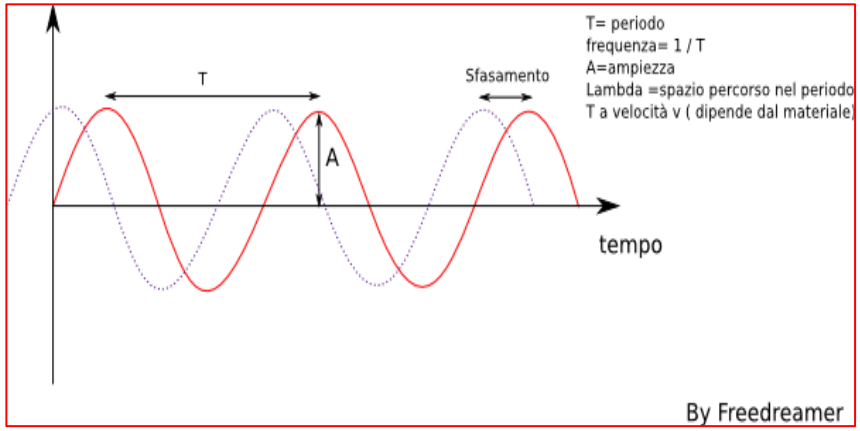

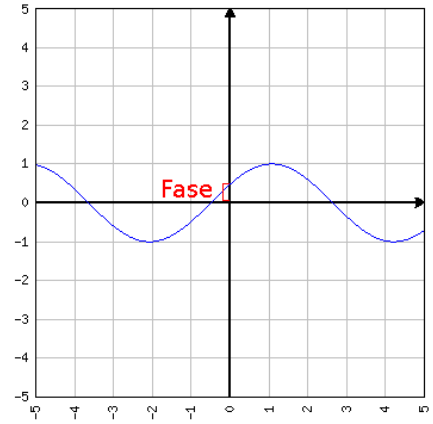

What is a wave?
«energy propagated through matter» A. Einstein

a)Angiografia dyeless basata ***sull'ampiezza*** del segnale OCT

b) Angiografia dyeless basata ***sulla fase*** del segnale OCT

c) Angiografia dyeless basata ***sull'ampiezza e sulla fase*** del segnale OCT (complex signal)

Algoritmi & network vascolare corio-retinico dyeless

- **OMAG**
- **Speckle Variance** «creare immagini a partire da macchie»
- **Phase Variance**
- **SSADA**
- **Correlation Mapping**

- **contrasto**
- **signal-to-noise ratio (SNR)**
- **tempi computazionali**
- **efficienza**
- **praticabilità informatico-tomografica**
- **capacità finale di resa iconografica**

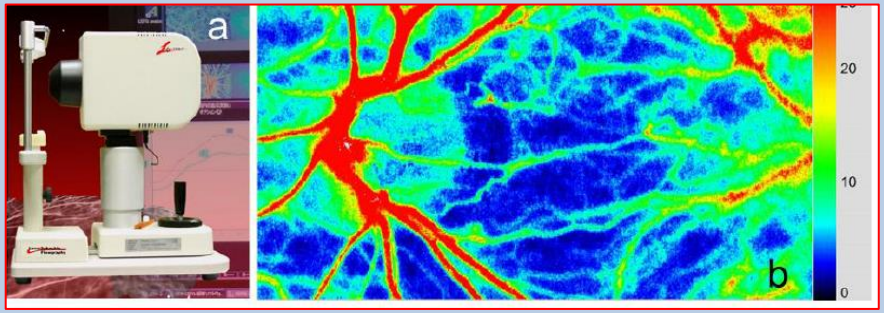

LSFG-NAVI-OPE Laser Speckle Flowgraphy

- R. K. Wang et al., “Depth-resolved imaging of capillary networks in retina and choroid using ultrahigh sensitive optical microangiography,” Opt. Lett. 35(9), 1467–1469 (2010).
- A. Mariampillai et al., “Speckle variance detection of microvasculature using swept-source optical coherence tomography,” Opt. Lett. 33(13),1530–1532 (2008).
- D. Yu Kim et al., “In vivo volumetric imaging of human retinal circulation with phase-variance optical coherence tomography,” Biomed. Opt. Express 2(6), 1504–1513 (2011).
- Y. Jia et al. “Split-spectrum amplitude-decorrelation angiography with optical coherence tomography” Opt. Express 20(4), 4710–4725 (2012).
- H. M. Subhash and M. J. Leahy, “Microcirculation imaging based on full-range high-speed spectral domain correlation mapping optical coherence tomography” J. Biomed. Opt. 19(2), 021103 (2014).

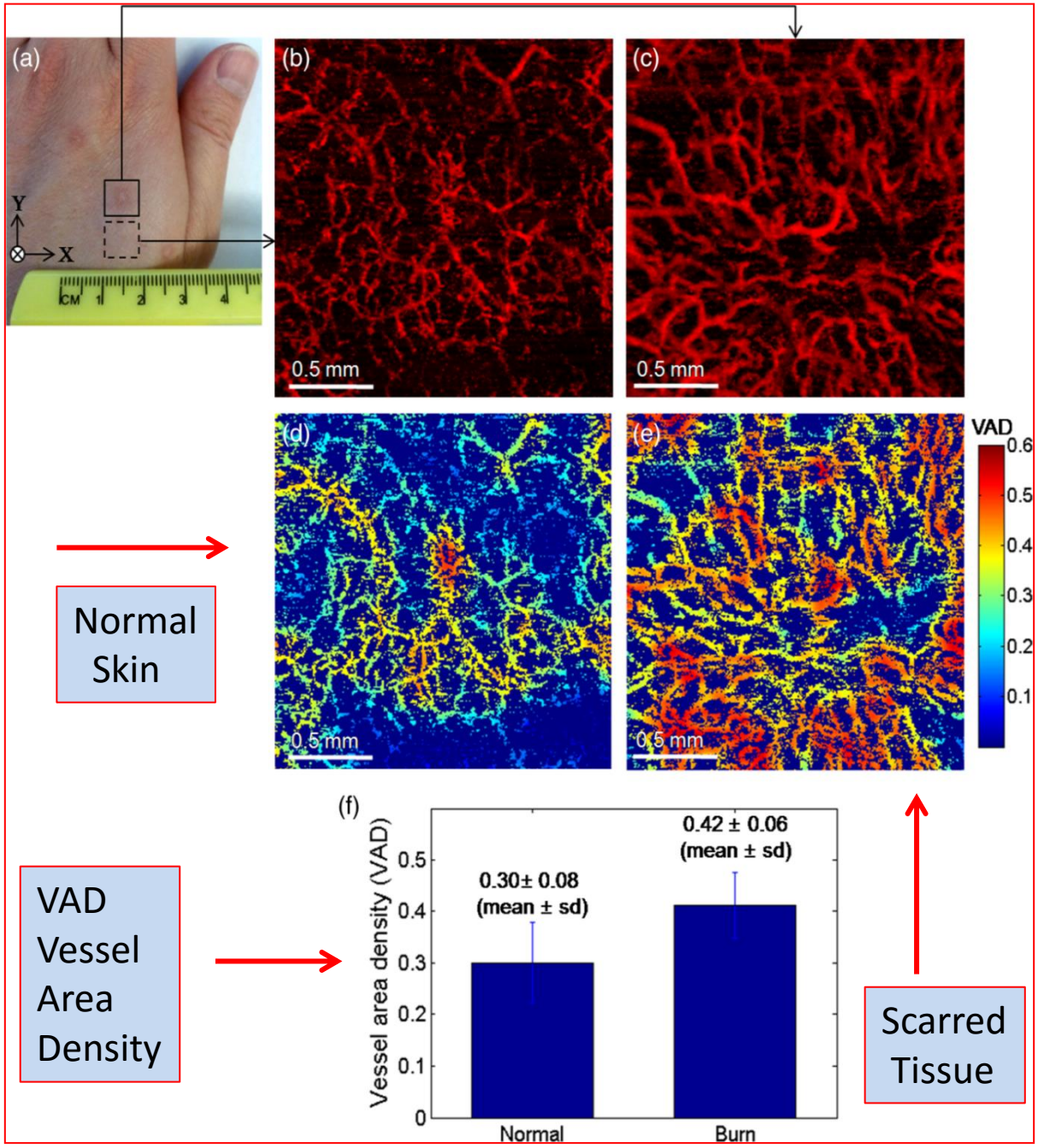

(a) Photograph of a 10 month-old scar due to a **laser burn** **(a solid box)** and an adjacent **normal skin** **(a dashed box)** on the left dorsal hand of a human subject.

(b) and (c) En face (XY) MIP (maximum intensity projection) view images [2.0 mm (X)×2.0 mm (Y)] of the vasculatures over a physical depth of **719 µm** below the surface of the **normal skin tissue** and the **scarred tissue.**

(d) and (e) Color-coded vessel density area maps of the **normal skin** and the **scarred tissue**, respectively, and their **mean and standard deviation values are represented as error bars in (f).**

by Woo June Choi J. Biomed. Opt 2014

The performance comparisons. (a)–(e) The ***blood vessel network in normal human retina*** visualized by optical microangiography ***(a) OMAG, (b) Speckle Variance, (c) Phase Variance, (d) SSADA),*** and ***(e) Correlation Mapping. (f)*** The capillaries selected as in yellow to evaluate the ***connectivity*** of the angiogram. by Anqi Zhang et al. J. of Biomedical Optics 20(10), 100901 (October 2015).

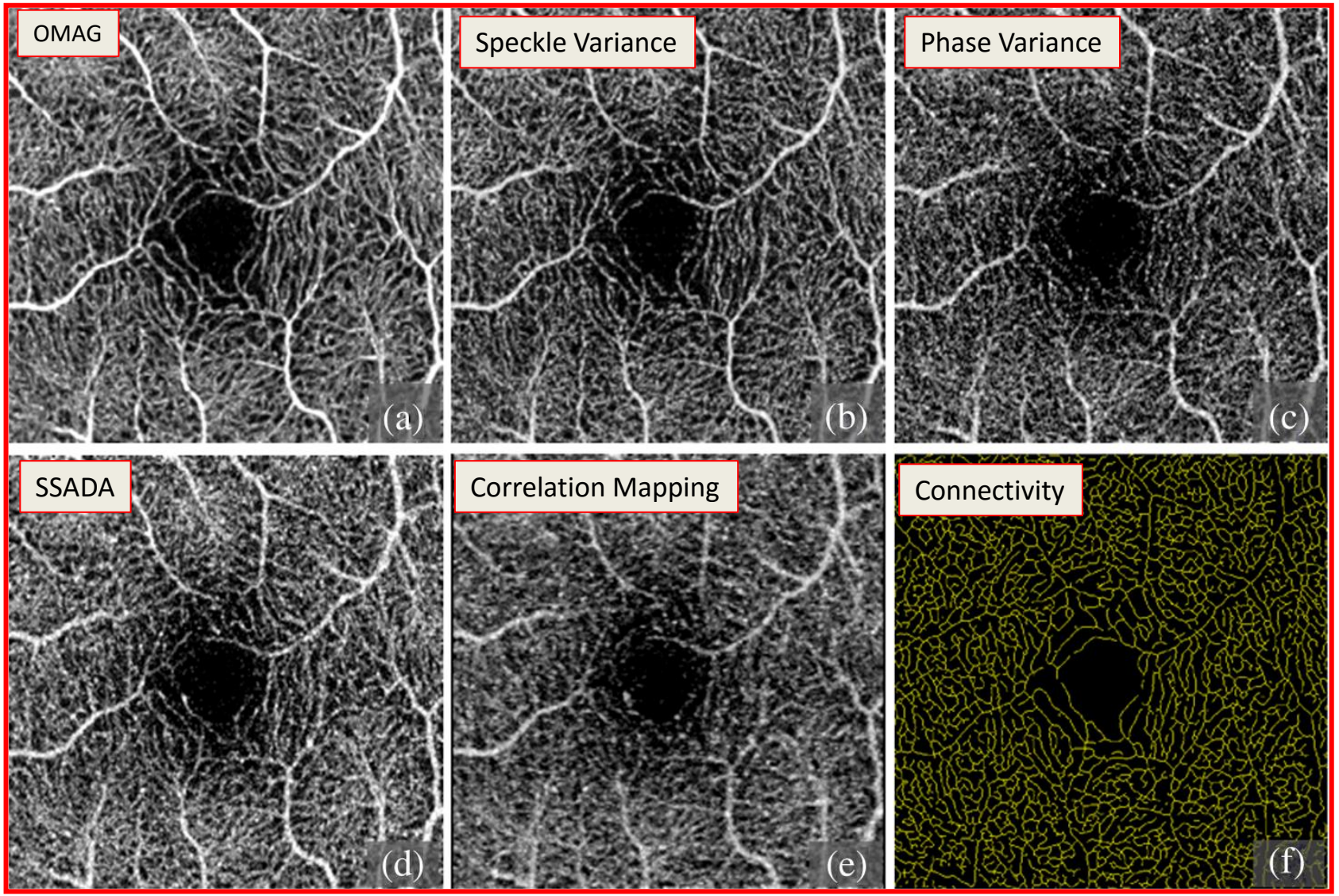

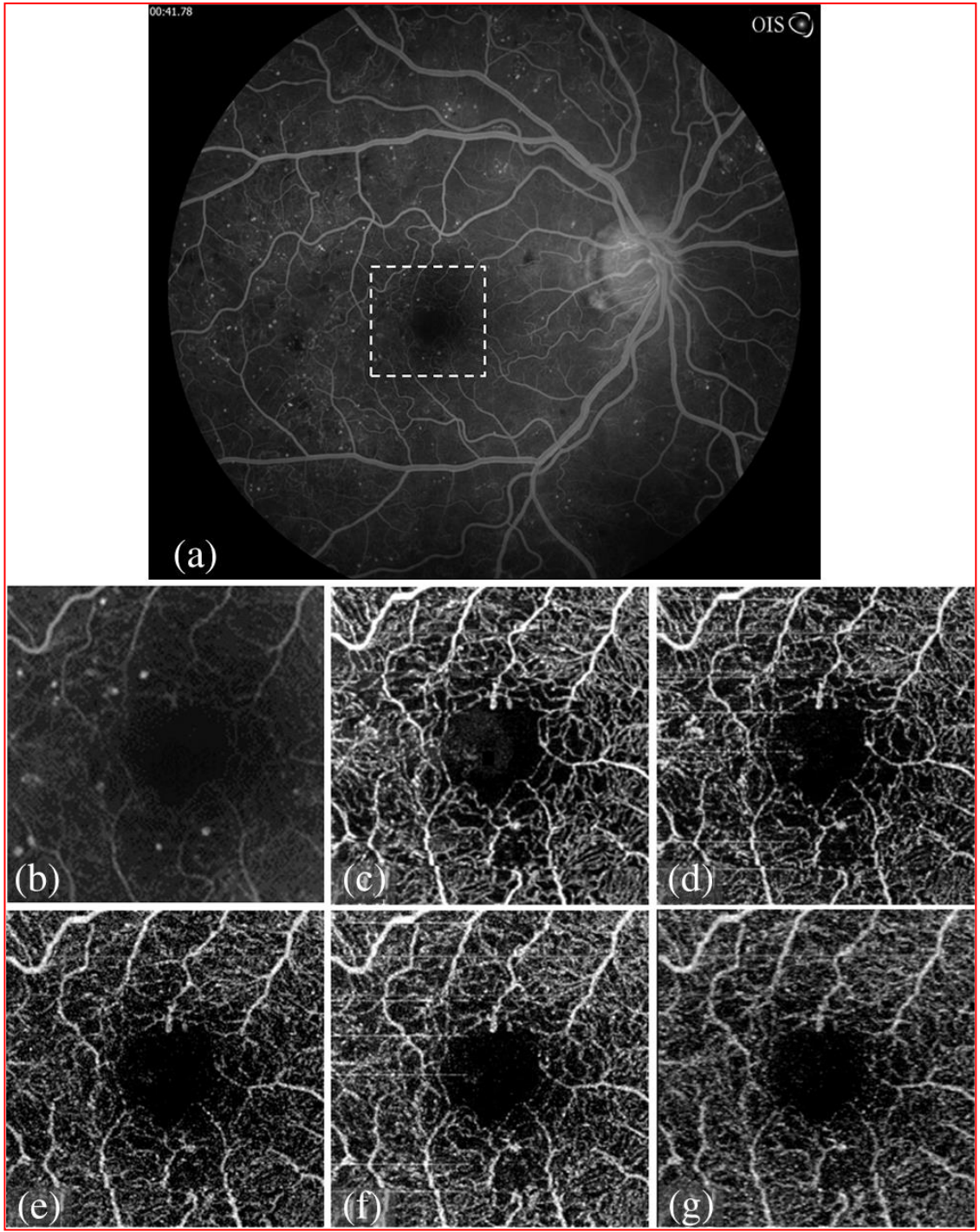

The performance comparisons using the dataset captured from a subject diagnosed with **diabetic retinopathy**.

(a) ***Fluorescein angiogram*** where the scanned area is marked with dashed square box ***3mm x 3mm***

(b) ***Zoomed fluorescein angiography*** image corresponding to the area for OCT angiography.

(c)→(g) The retinal blood vessel network visualized by

OMAG → **(c)**
Speckle Variance → **(d)**
Phase Variance → **(e)**
SSADA → **(f)**
Correlation Mapping → **(g)**

da Anqi Zhang et al. Journal of Biomedical Optics 20(10), 100901 (October 2015).

AngioPlex™ Technology
Principio di funzionamento: uso dell'algoritmo OMAG

AngioPlex ™ Technology

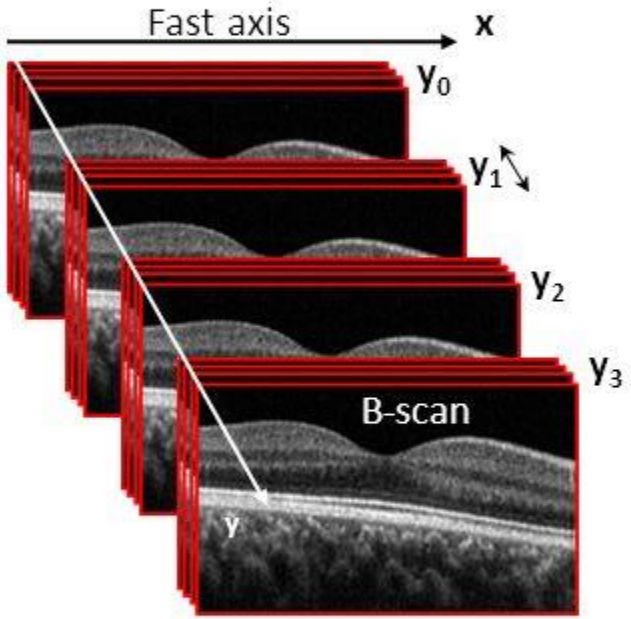

AngioPlex Maps

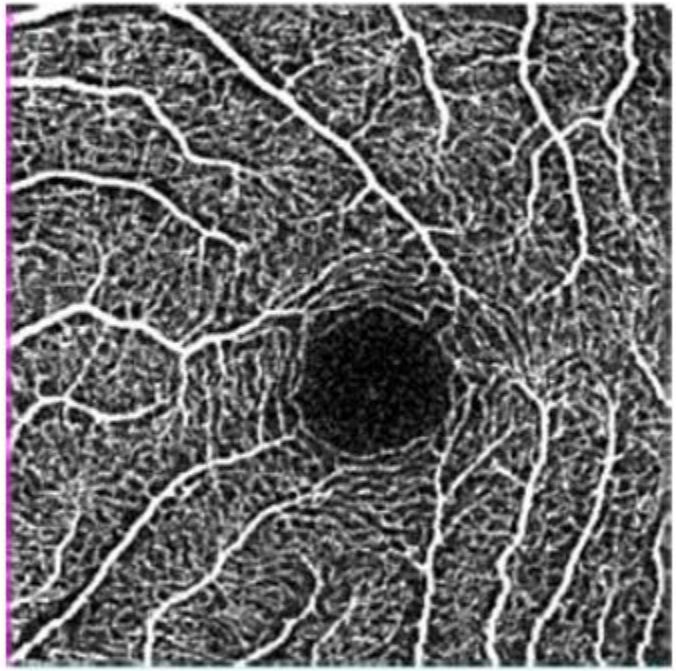

La tecnologia di AngioPlex ™ evidenzia il moto di corpuscoli quali i globuli rossi all'interno di una sequenza di B-scan OCT acquisite ripetutamente nella stessa posizione della retina.

AngioPlex ™ consente di ricostruire mappe della rete microvascolare perfusa all'interno della retina e della coroide.

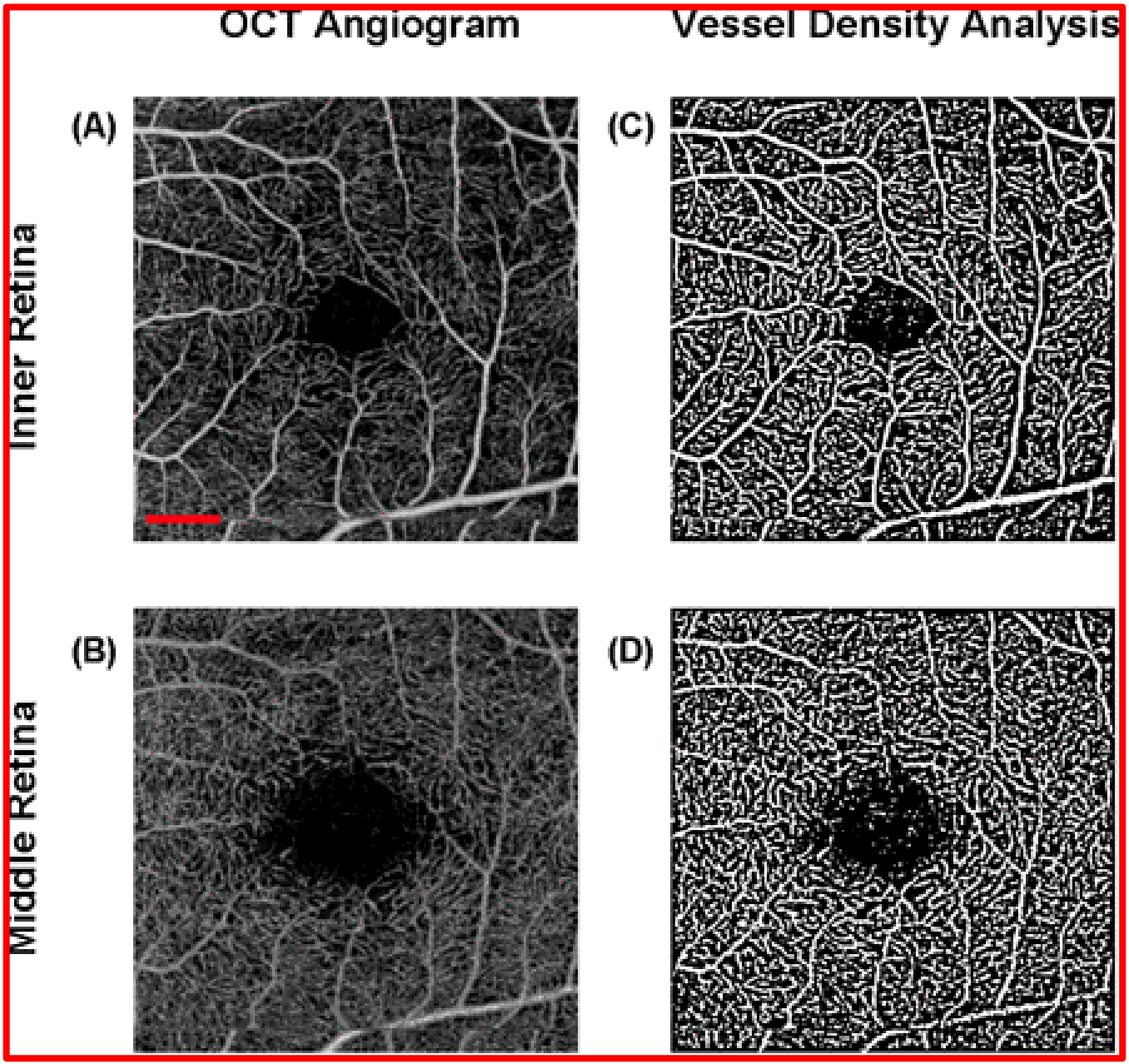

iovs investigative ophthalmology & visual science
an ARVO journal

Vessel density analysis of the central macular region of a healthy subject yielded an average total density of:

31.68% ± 1.15%
in the **inner retina**

and a density of:

30.86% ± 1.20%
in the **middle retina**

by Jack Yi, ARVO 2015

Data was acquired using a Cirrus (Carl Zeiss Meditec, Dublin, CA) SS-OCT and SD-OCT prototype angiography systems.

The **parafoveal** and **foveal** regions were outlined with **circles of diameters of 2.5mm and 1.5mm**; vessel density was calculated for central foveal region (FAZ excluded) and in quadrants for parafovea

Cirrus HD-5000 OCTangiography prototype using OMAG by Zhongdi Chu et al ARVO 2015

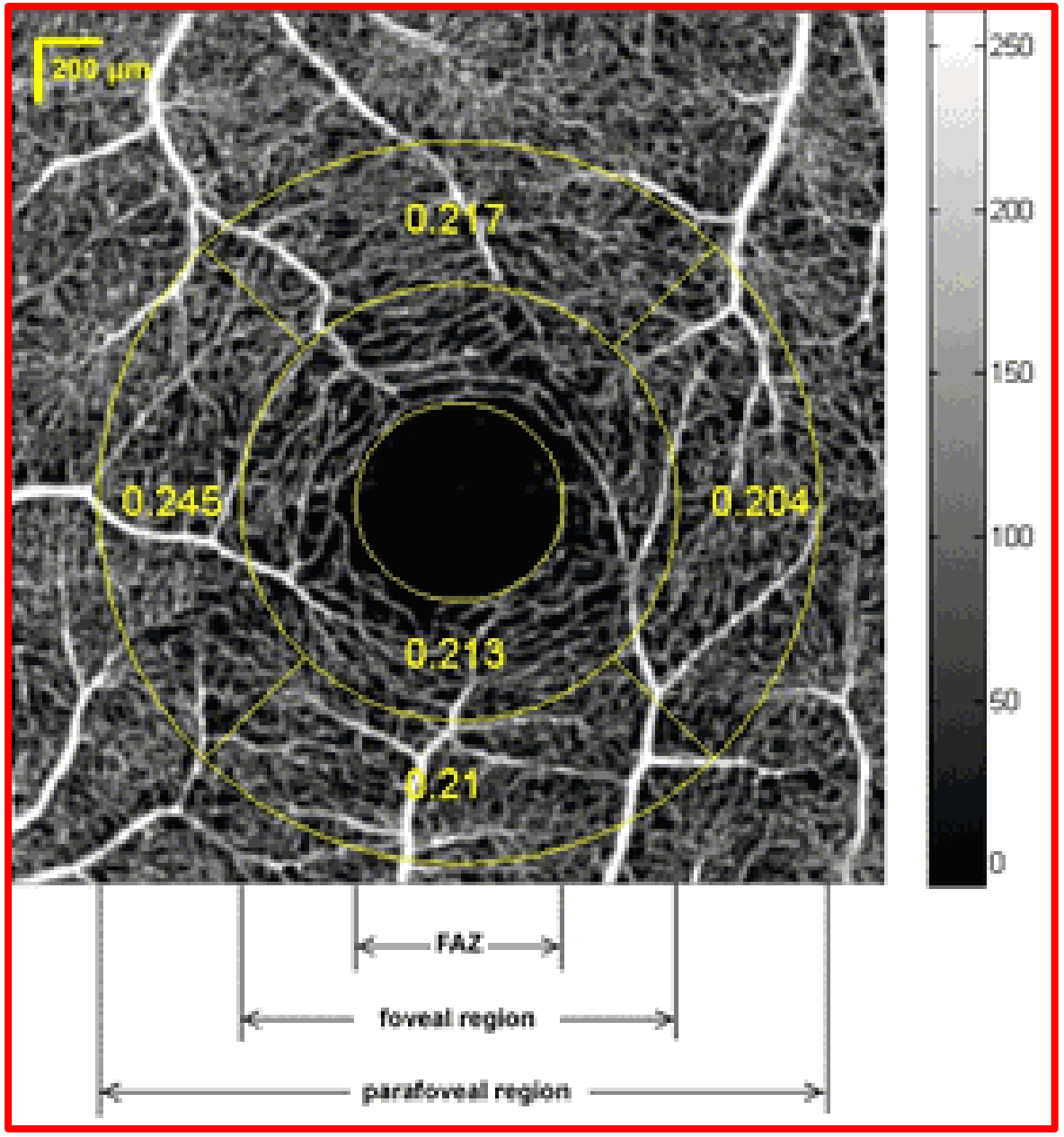

iovs investigative ophthalmology & visual science
an ARVO journal

by Yi-Sing Hsiao et al. 2015

ROI Regions of Interest
MIP Maximum Intensity Projection
COV Coefficient of Variation

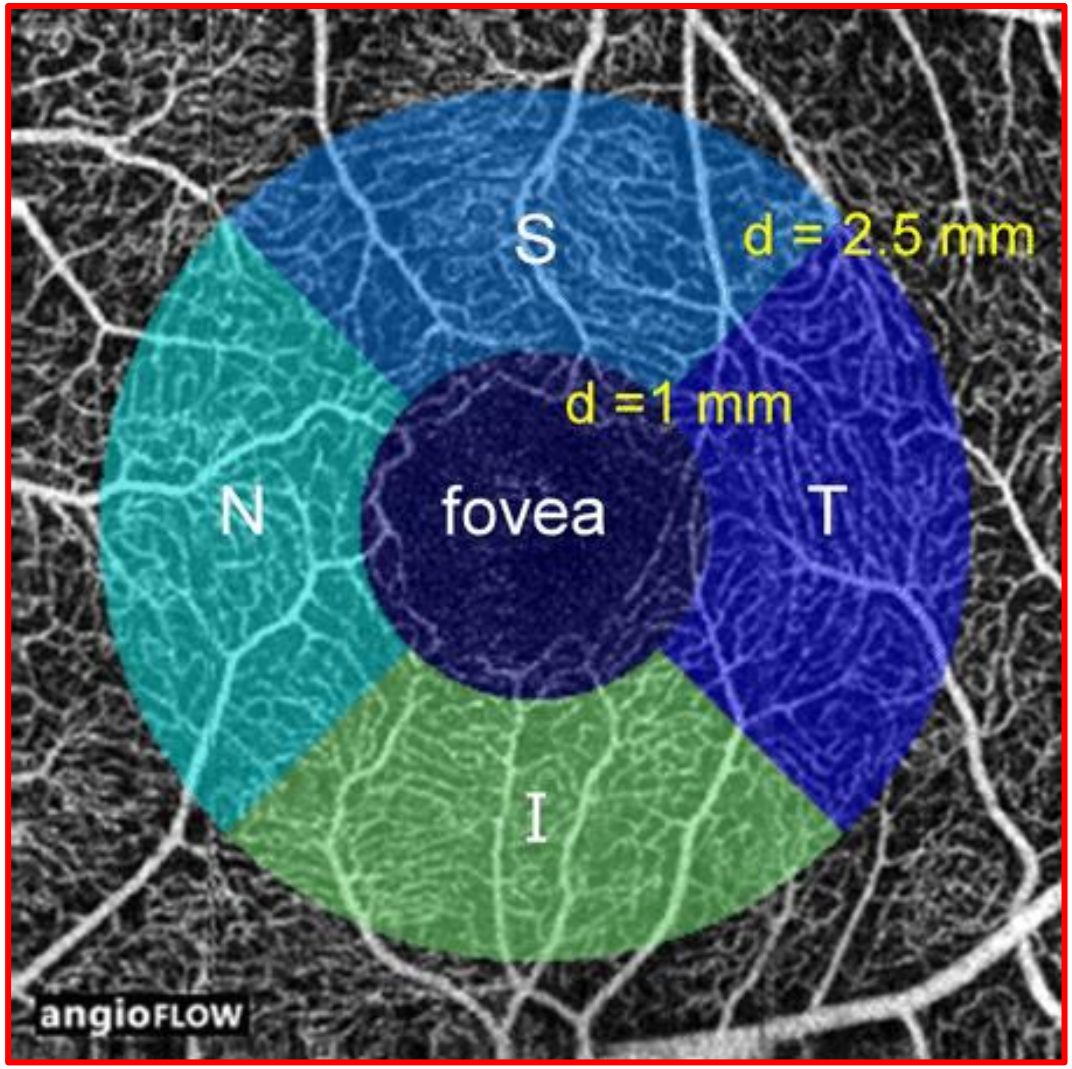

Table 1. Vessel length density

Layer		Superficial		Deep	
Projection		Avg	MIP	Avg	MIP
Vessel length density [S.D.] (mm^{-1})					
ROI	3 x 3 mm^2	19.23 [1.66]	21.75 [1.56]	24.65 [1.50]	25.45 [1.60]
ROI	T	20.35 [2.07]	22.80 [1.95]	25.49 [1.96]	26.22 [1.93]
ROI	S	21.33 [2.05]	24.71 [2.04]	27.58 [1.81]	28.17 [2.08]
ROI	N	20.67 [1.65]	23.36 [1.46]	25.61 [1.55]	26.72 [1.67]
ROI	I	21.03 [1.88]	24.40 [2.02]	27.20 [1.60]	27.86 [1.94]
Average COV (%)					
ROI	3 x 3	4.49	4.38	3.12	3.28
ROI	T	4.99	3.81	3.55	3.47
ROI	S	5.76	5.47	4.29	5.12
ROI	N	4.60	4.42	3.17	3.97
ROI	I	5.56	6.13	4.13	4.50

Table 2. Fovea avascular zone area

Layer	Superficial		Deep	
Projection	Avg	MIP	Avg	MIP
FAZ (mm^2) [S.D.]	0.358 [0.084]	0.385 [0.080]	0.584 [0.150]	0.496 [0.113]
Repeatability/ S.D. (mm^2)	0.029 [0.027]	0.028 [0.014]	0.036 [0.013]	0.039 [0.021]
Avg.COV(%)	8.953	7.862	6.609	8.172

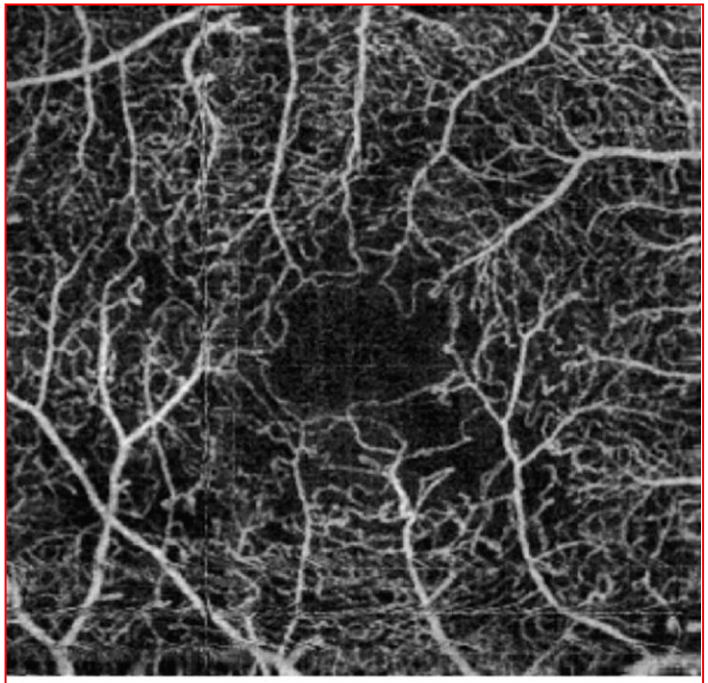

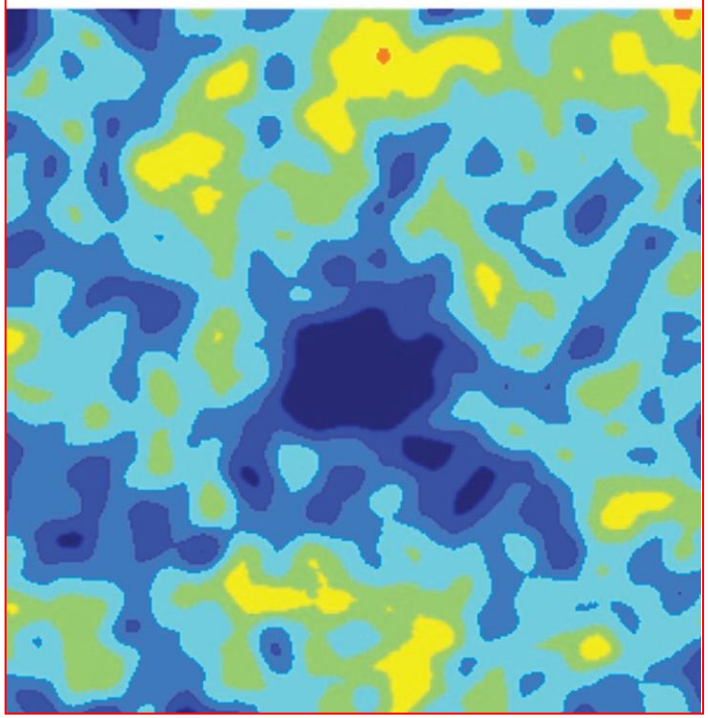

Average perfusion density for the **control group** was

0.2477 ±0.0639

(3x3)

0.2702 ±0.1006

(6x6)

Average perfusion density for the **NPDR group** was significantly reduced at

0.2012 ±0.0694

(3x3)

0.2474 ±0.1048

(6x6)

The **PDR group** appeared futher reduced at

0.1944 ±0.0692

(3x3)

0.2402 ±0.1047

(6x6)

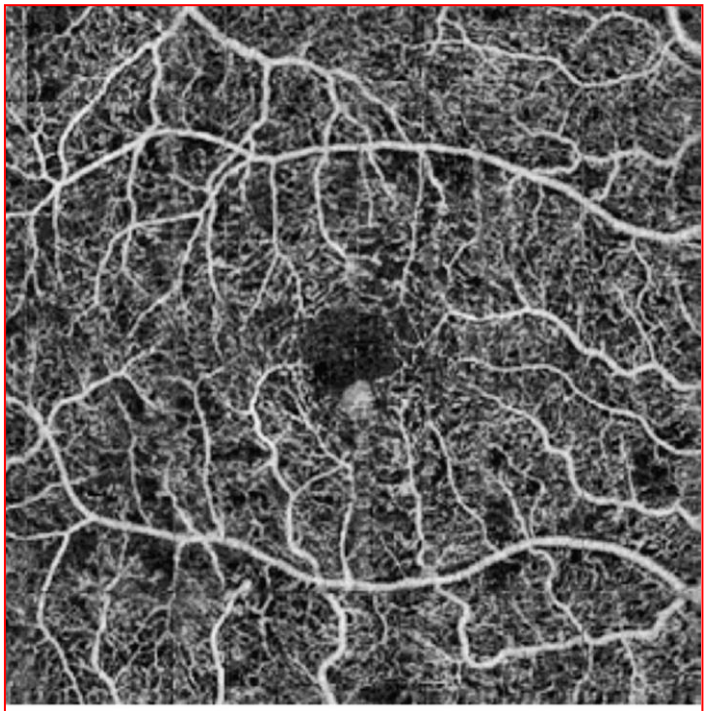

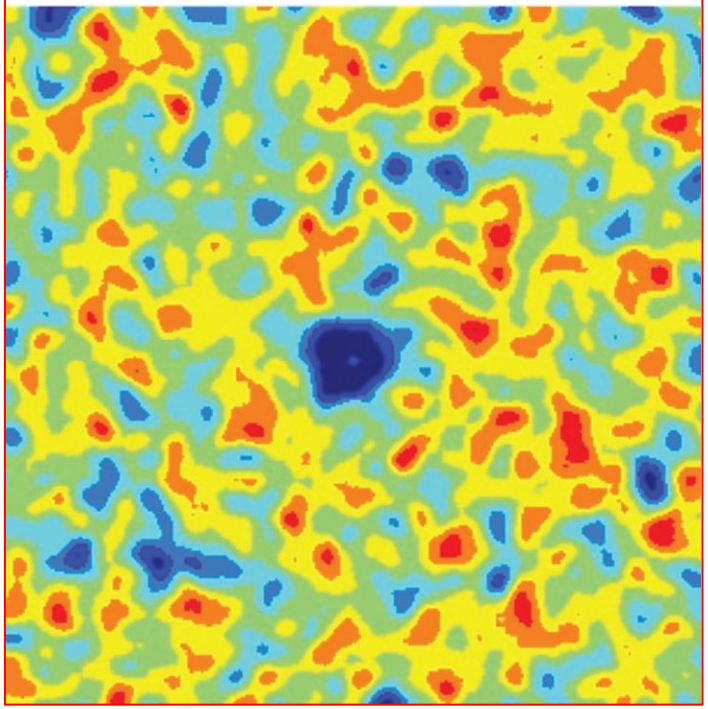

OCT angiography demonstrates an enlarged, irregular perifoveal capillary network in a patient with nonproliferative diabetic retinopathy. Multiple microaneurysms (arrows) and vascular loops are seen. Nonperfused areas are highlighted in yellow, enabling calculation of a ratio of perfusion. by Ching J. Chen et al ARVO 2015

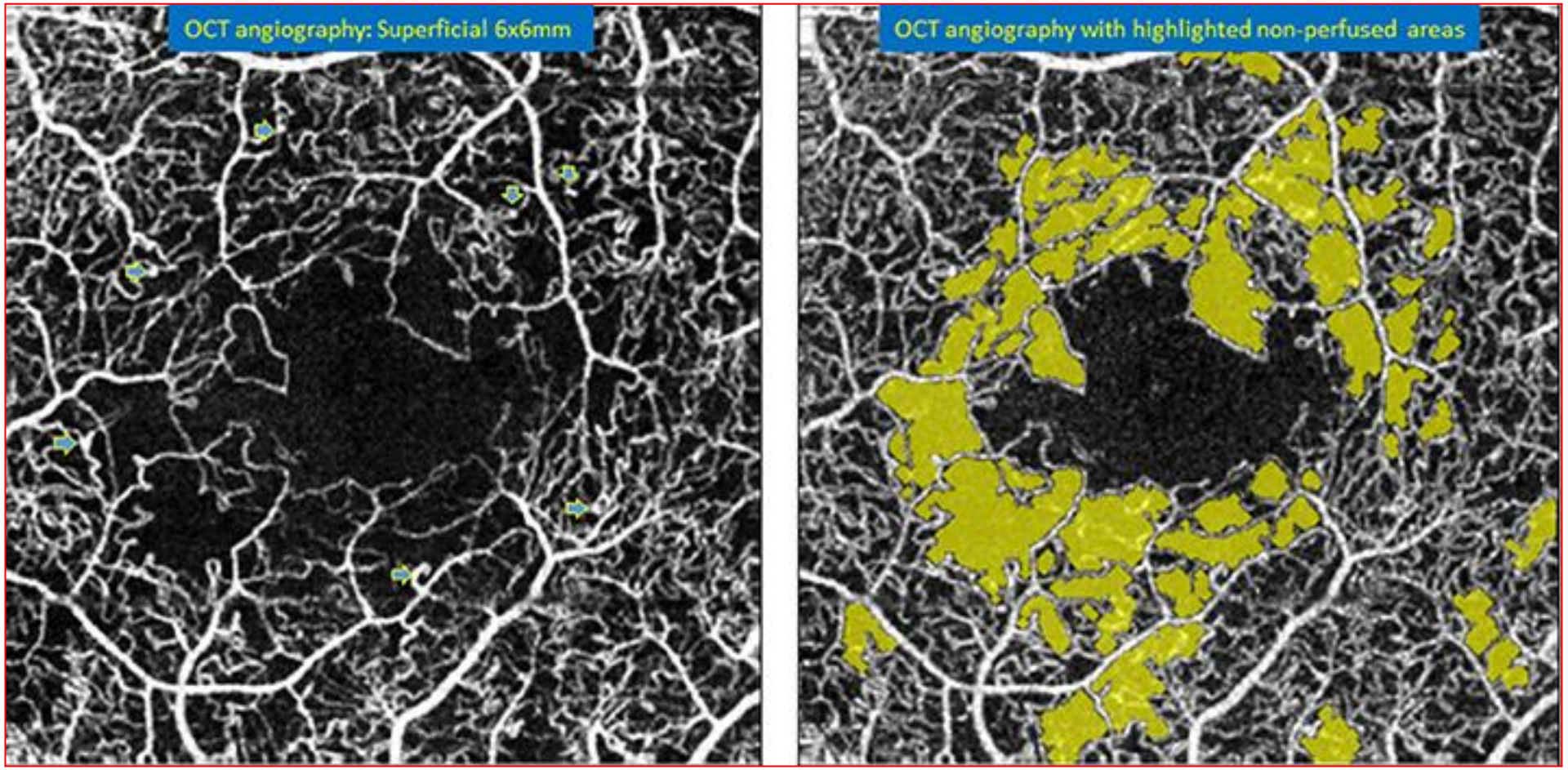

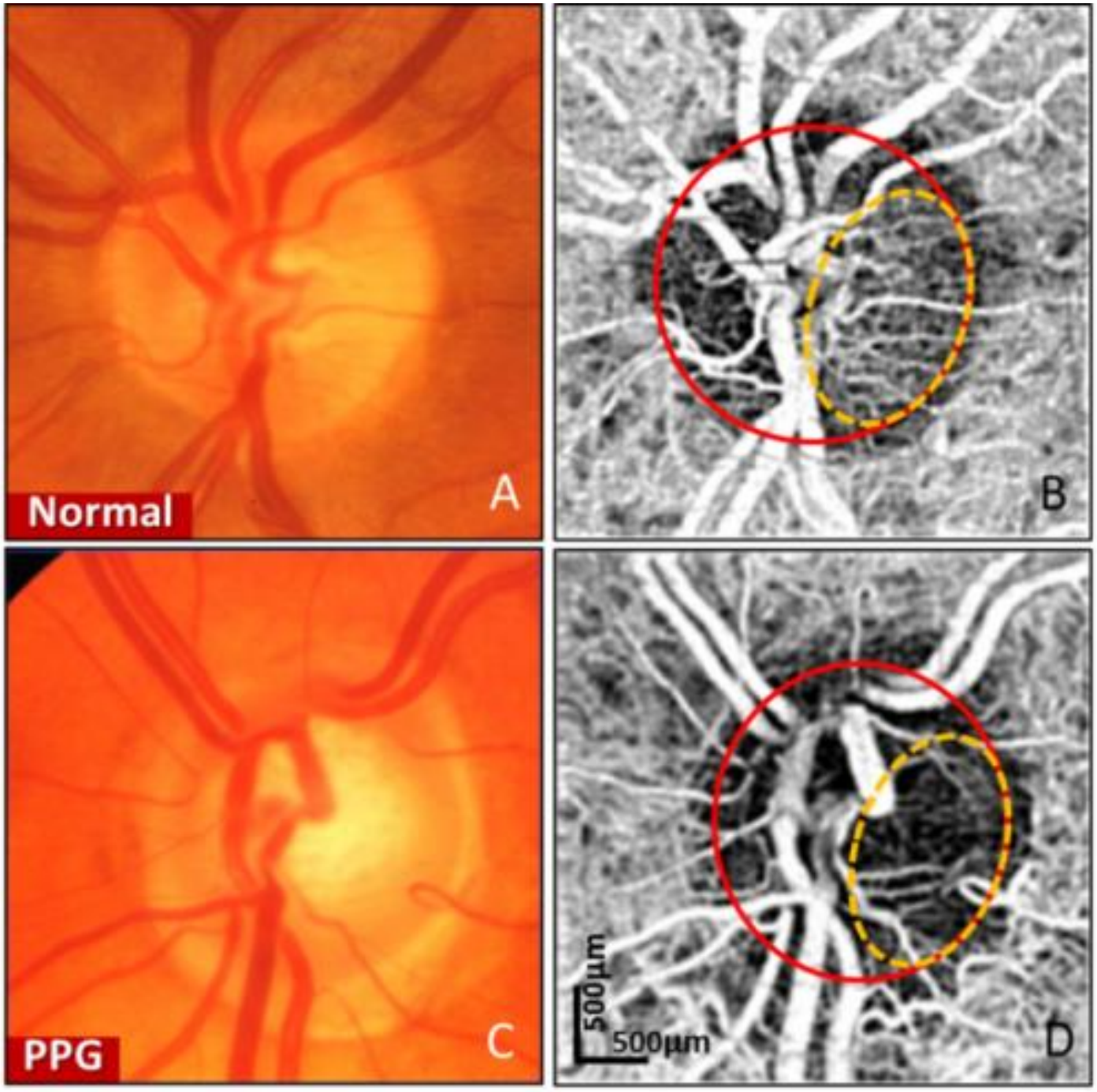

***- Disc photographs* (A, C)**
***- En face OCT angiograms* (B, D)**

***- ONH normal* (A, B)**

***- Preperimetric glaucoma (PPG)* (C, D)**

Both examples are from ***left eyes.***

In (B) and (D) the ***solid circles*** indicate the **whole discs,** and the ***dash circles*** indicate the **temporal ellipses.**
A dense microvascular network was visible on the OCT angiography of the ***normal disc* (B).**
This network was greatly attenuated in the ***glaucomatous disc* (D)**

by Yali Jia et al

Right eye of a normal subject *(A1-H1)* and, the left eye of a perimetric glaucoma subject *(A2-H2)*

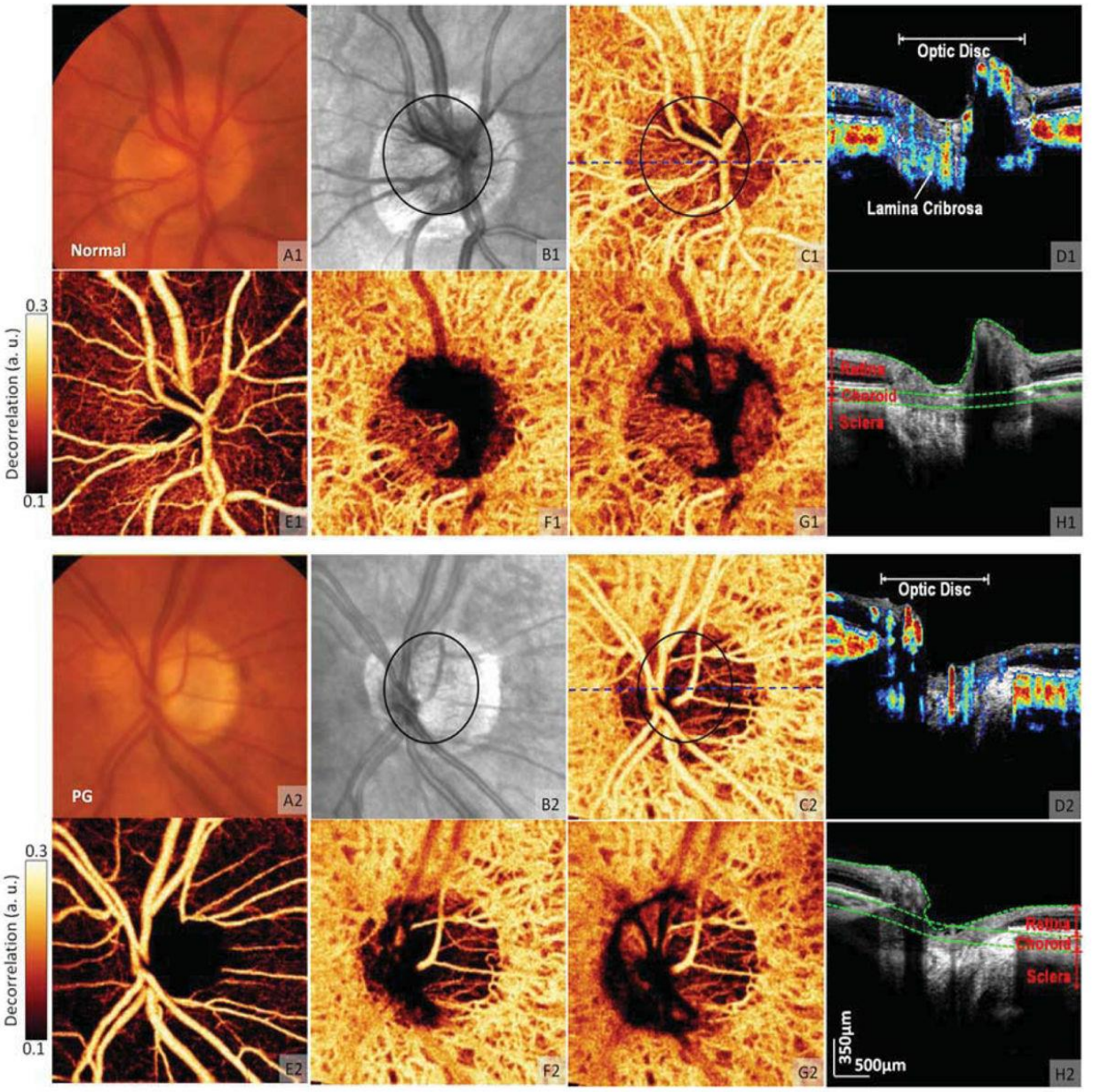

-**Disc photographs** ***(A1, A2)***
(OCT) reflectance ***(B1, B2)***
-***whole depth OCT*** angiograms ***(C1, C2)***
-***cross-sectional*** angiograms ***(D1, D2)***
in gray scale
A dense microvascular network was visible on the OCT angiography of the ***normal disc*** ***(C1)***
This network was greatly attenuated in the ***glaucomatous disc*** ***(C2)***
en face maximum projection in 3 layers

retinal angiograms ***(E1, E2)***
choroidal angiograms ***(F1, F2)***
scleral/lamina cribrosa angiograms ***(G1,G2)***

by Yali Jia et al, Ophthalmology 2014
SS-OCT and SSADA

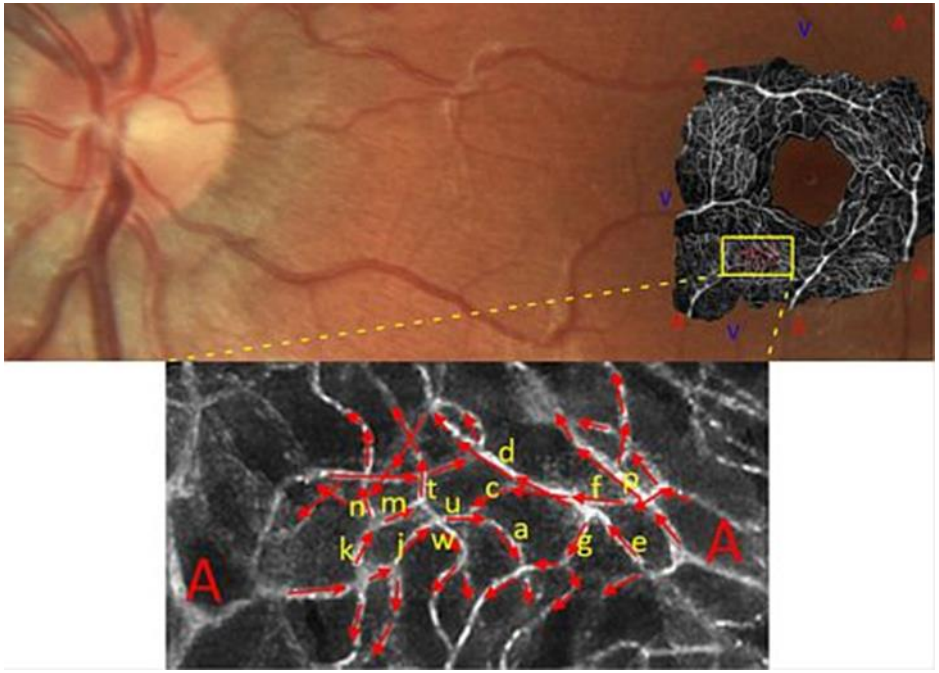

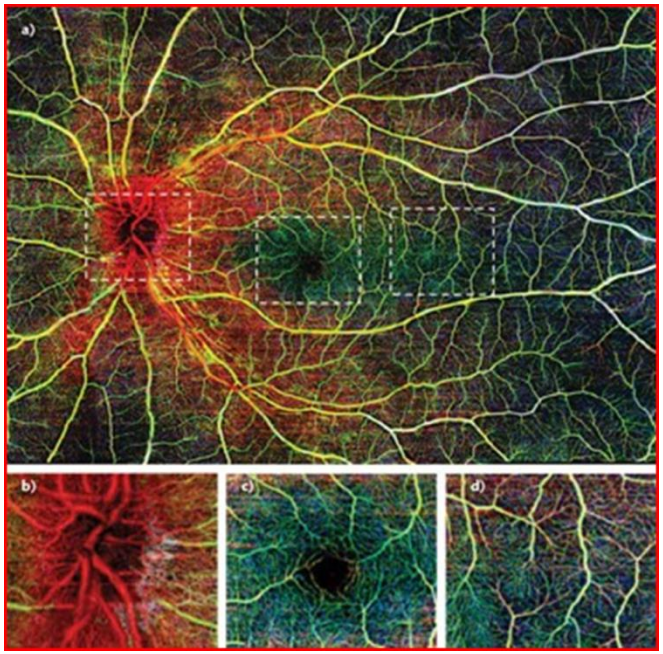

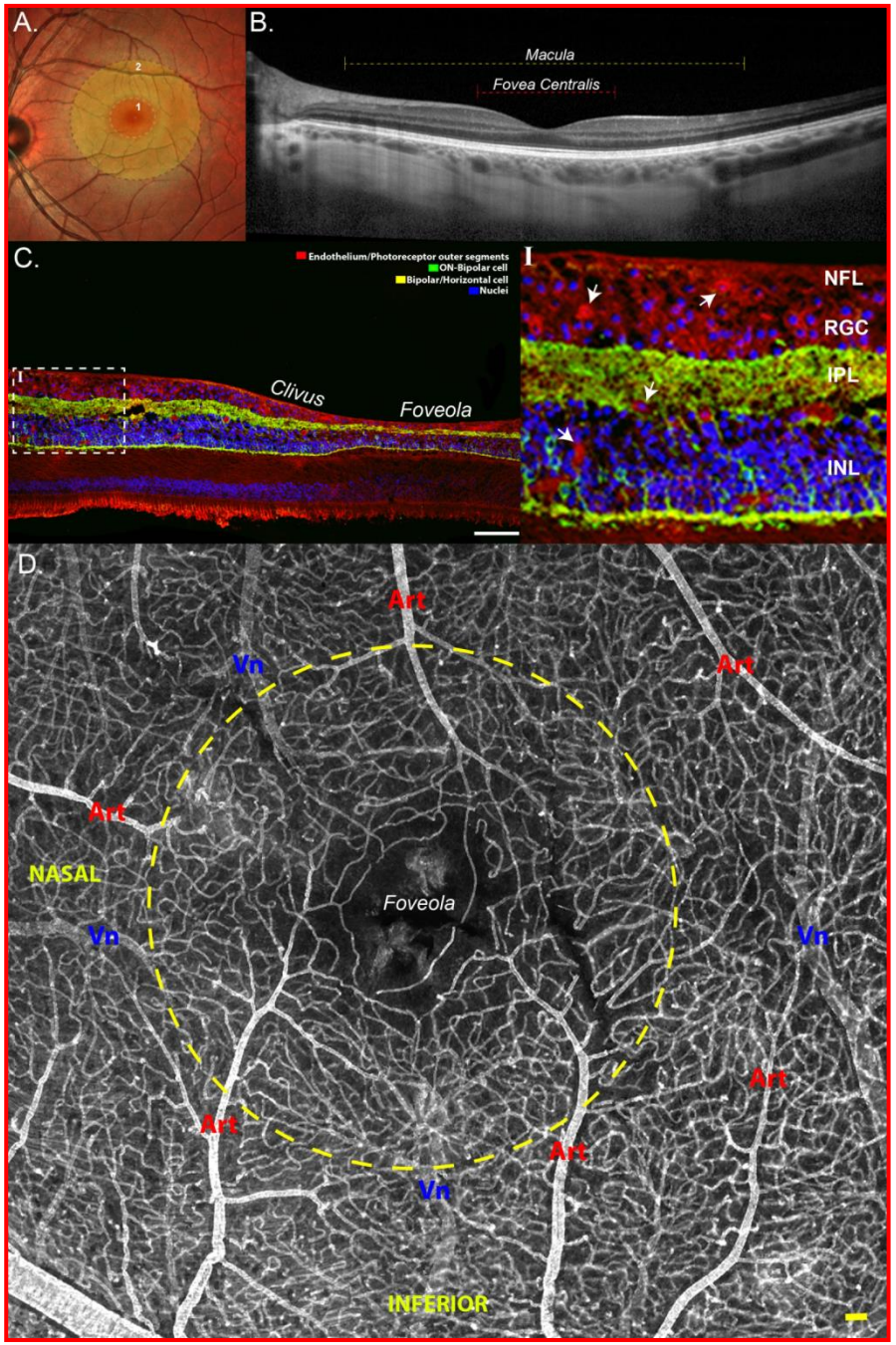

svOCT (1060-nm, 100-kHz custom-built system)

Galileo Galilei, padre della scienza moderna
(Pisa, 15 febbraio 1564 – Arcetri, 8 gennaio 1642)

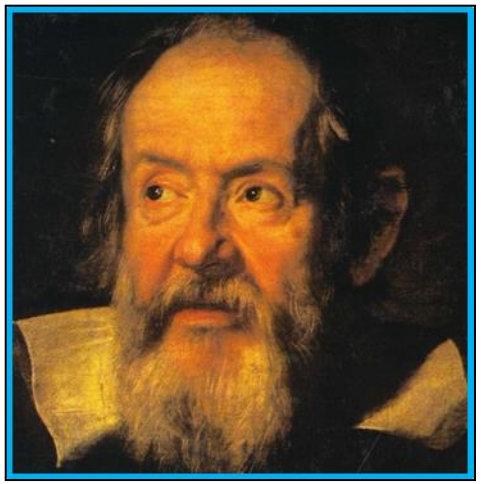

Misura ciò che è misurabile, e rendi misurabile ciò che non lo è

Galileo mostra il telescopio: al cospetto del Senato Veneziano, lo scienziato mostrò il funzionamento del primo telescopio rifrattore della storia, **25 agosto 1609**

Thank you for your kind attention!